Supporting Information

Crystallographic and Theoretical Insights into a Fluorogenic Turn-On Probe for Selective Fe^{3+} Detection with Biomolecular Binding and In Vitro Anticancer Studies

Hazeena Shinziya[a, b], Avijit Kumar Das*[a,b],Sahana Suresh[a, b], Urmila Saha[c], Gouri Karan[d], Sujata Maiti Choudhury[d], Paula Brandao[e] and Malay Dolai*[f]

[a] Department of Chemistry, Christ University, Hosur Road, Bangalore, Karnataka, 560029 India

*Email: avijitkumar.das@christuniversity.in, sanjuavi.das@gmail.com

[b]Centre for Renewable Energy and Environmental Sustainability, Christ University, Karnataka, 560029, India

[c] Department of Chemistry, Indian Association for the Cultivation of Science, Raja SC Mullick Road, Kolkata 700032, WB, India

[d]Cancer Nanotherapeutics Laboratory, Biochemistry, Molecular Endocrinology, and Reproductive Physiology Division, Department of Human Physiology, Vidyasagar University, Midnapore- 721 102, West Bengal, India.

[e]Department of Chemistry, CICECO, University of Aveiro, 3810-193 Aveiro, Portugal

[f]Department of Chemistry, Prabhat Kumar College (Vidyasagar University), Purba Medinipur 721404, WB, India. E-mail: dolaimalay@yahoo.in

1. Experimental

1.1. General:

Unless otherwise mentioned, chemicals and solvents were purchased from Sigma-Aldrich Chemicals Private Limited and were used without further purification. ^{1}H-NMR spectra were recorded on Bruker 400 MHz instrument. For NMR spectra, DMSO was used as solventusing TMS as an internal standard. Chemical shifts are expressed in δ- units and ^{1}H–^{1}H and ^{1}H–C coupling constants in Hz. UV-*vis* titration experiments were performed on a UV-Spectrophotometer: PerkinElmer, Lambda 30 and a fluorescence experiment was done using Shimadzu RF-6000 Fluorescence spectrofluorometer using a fluorescence cell of 10 mm path.

1.2 General method of UV-*vis* and fluorescence titration:

By UV-*vis* method:

For UV-*vis* titrations, a stock solution of the sensor **HMC** was prepared (c = 2 x 10^{-5}M) in CH_3CN-HEPES buffer (9:1 v/v, pH = 7.4).The solution of the guest interfering analytes like Cu^{2+}, Mn^{2+}, Pb^{2+}, Cd^{2+}, Fe^{2+}, Cu^{2+}, Fe^{3+}, Zn^{2+}, Co^{2+}, Al^{3+}, Fe^{3+}, Ni^{2+} as their chloride salts were also prepared in the order of (c = 2×10^{-4}M). Solutions of various concentrations containing the sensor and increasing concentrations of cations were prepared separately. The spectra of these solutions were recorded by means of UV-*vis* methods.

For UV-*vis* titrations of **HMC** with ct-DNA, BSA, the stock solution of the sensor (c = 2× 10^{-5} M) was prepared in DMSO- Tris-HCl buffer (40 µL in 2 ml Tris-HCl buffer) at pH 7.2. And tris-HCl buffer was used to prepare the solution of ct-DNA (c = 2 mM in base pairs), BSA (c = 7.4 µM). The spectra of these solutions were recorded by means of UV-*vis* methods.

By fluorescence method:

For fluorescence titrations, a stock solution of the sensor (c = 2 x 10^{-5}M) was prepared for the titration of cations in CH_3CN-HEPES buffer (9:1, v/v, pH = 7.4). The solution of the guest cations using their chloride salts in the order of 200 µM was also prepared. Solutions of various concentrations containing the sensor and increasing concentrations of cations were prepared separately. The spectra of these solutions were recorded by means of fluorescence methods.

For fluorescence titrations of **HMC** with ct-DNA, BSA, the stock solution of the sensor (c = 2× 10^{-5} M) was prepared in DMSO- Tris-HCl buffer (40 µL in 2 ml Tris-HCl buffer) at pH 7.4. Tris-HCl buffer was used to prepare the solution of ct-DNA (c = 2 mM in

base pairs), BSA (c = 7.4 μM). The spectra of these solutions were recorded by means of UV-*vis* methods.

UV-*vis* studies of HMC with Fe^{3+}

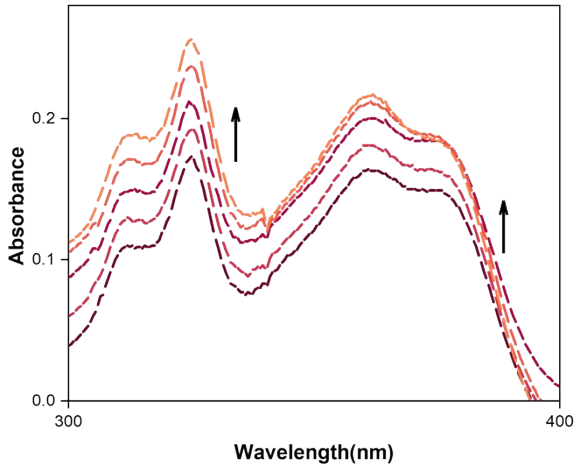

Figure S1: UV-*vis* absorption spectra of HMC (c= 2×10^{-5} M) with the incremental addition of Fe^{3+} (c = 2×10^{-4} M).

Fluorescence studies of probe HMC alone with ct-DNA

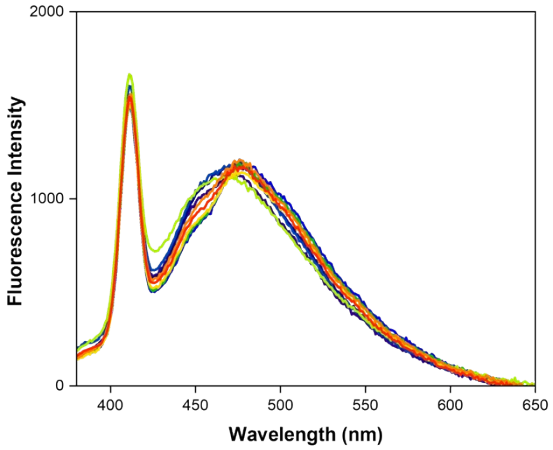

Figure S2: Fluorescence titration spectra of probe HMC (c = 2×10^{-5} M) with ct-DNA

2. Binding constant determination:

The binding constant value of cation Fe^{3+} with the sensor has been determined from the emission intensity data following the modified Benesi–Hildebrand equation, $1/\Delta I = 1/\Delta I$ max + (1/K[C]) ($1/\Delta I$ max). Here, $\Delta I = I\text{-}I_{min}$ and $\Delta I_{max} = I_{max}\text{-}I_{min}$, where I_{min}, I, and Imax are the emission intensities of the sensorconsidered in the absence of guest, at an intermediate concentration and at a concentration of complete saturation of guest, where K is the binding

constant and [C] is the guest concentration, respectively. From the plot of (Imax-Imin)/(I-Imin) against $[C]^{-1}$ for the sensor, the value of K has been determined from the slope. The binding constant (K_a) as determined by the fluorescence titration method for the sensor with Fe^{3+} is found to be $1x10^6$ M^{-1} (error < 10%).

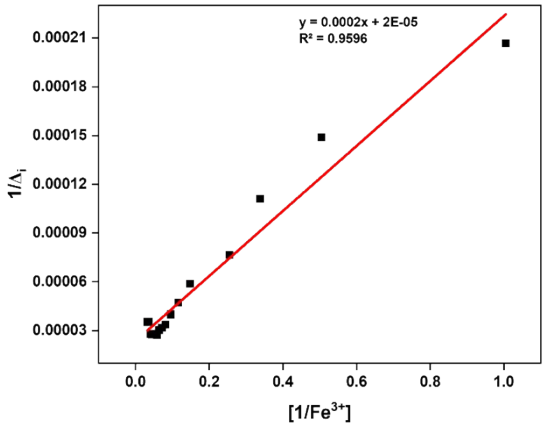

Figure S3. Benesi–Hildebrand plot from fluorescence titration data of receptor (20μM) with Fe^{3+} [G].

3. Calculation of the detection limit (DL):

The detection limit DL of **HMC** with Fe^{3+} was determined from the following equation:

$DL = K* Sb_1/S$

Where K = 2 or 3 (we take 3 in this case); Sb_1 is the standard deviation of the blank solution; S is the slope of the calibration curve.

From the graph Fig.S4, we get slope = 1959.3, Sb_1 value is 1218.351

for Fluorescence spectroscopy. Using the formula, we obtain a Detection Limit of 1.86 μM for Fe^{3+} using fluorescence spectroscopy.

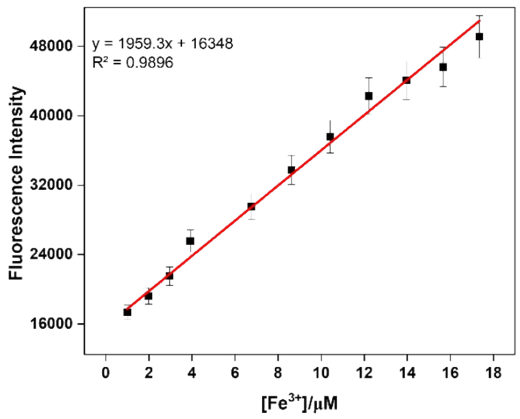

Figure S4. Changes of Fluorescence Intensity and absorbance of **HMC** as a function of $[Fe^{3+}]$ at 477 nm.

The detection limits (DL) of **HMC** with ct-DNA and BSA were determined from the following equation:

$DL = K^* Sb_1/S$

Where K = 2 or 3 (we take 3 in this case); Sb_1 is the standard deviation of the blank solution; S is the slope of the calibration curve.

From fluorescence titration of **HMC** with (a) ct-DNA and (b) BSA (Fig.S5), slope values are 58.391, 44780 and Sb_1values are 95.877,71.513 respectively.

The detection limits of **HMC** with ct-DNA were calculated to be 4.92μM and 4.8×10^{-3} μM for fluorescence spectroscopy.

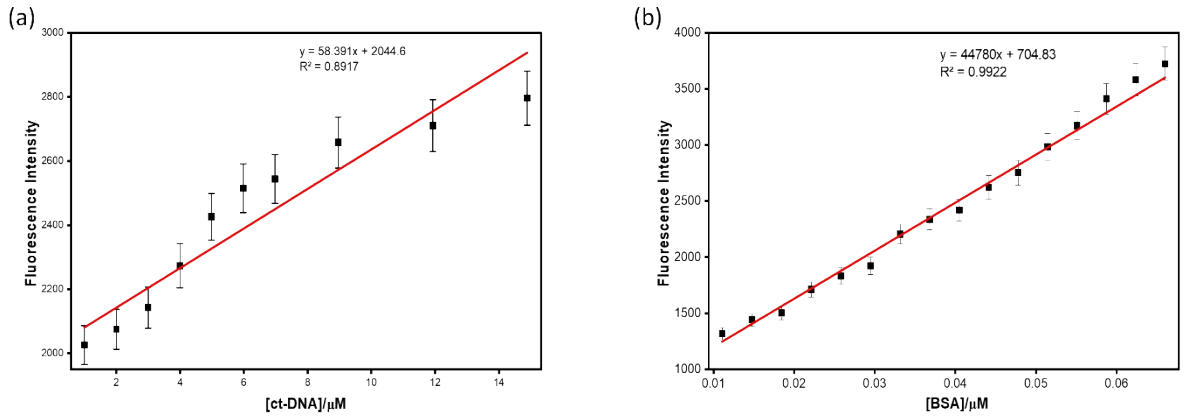

Figure S5. Changes of emission of **HMC** ($c = 2.0 \times 10^{-5}$ M) upon addition of (a) ct-DNA (c = 2mM in base pairs), (b) BSA (c = 7.4μM). (Error bar < 4%).

4. NMR and Mass spectra

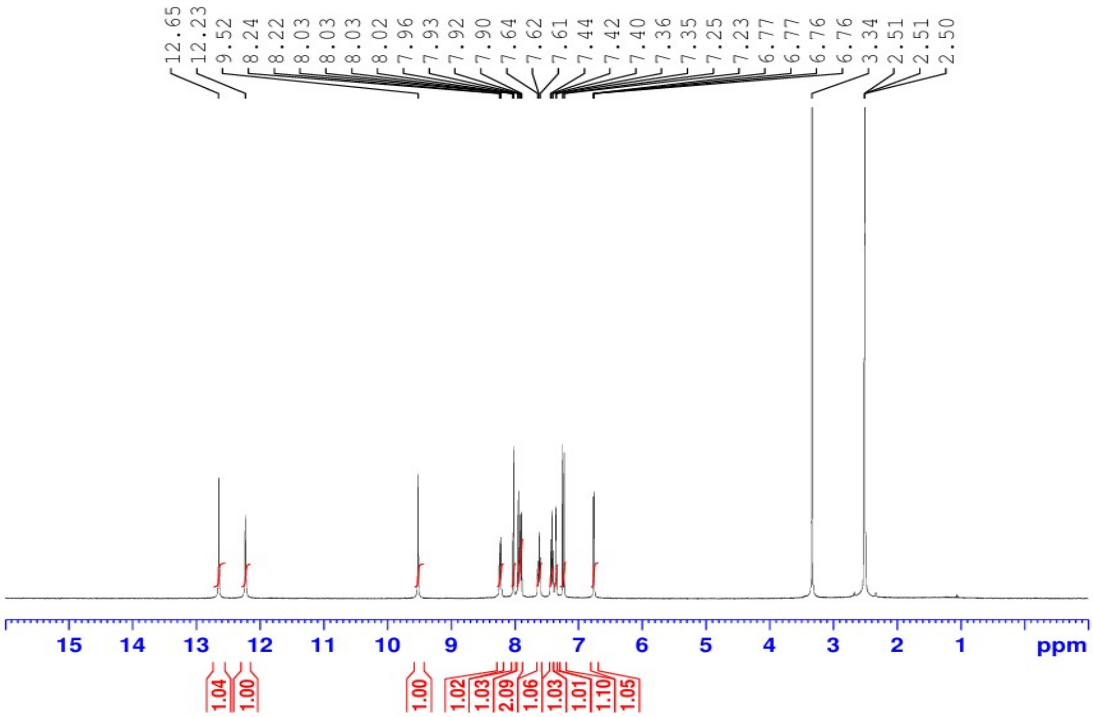

Figure S6: ^{1}H NMR spectrum of **HMC**

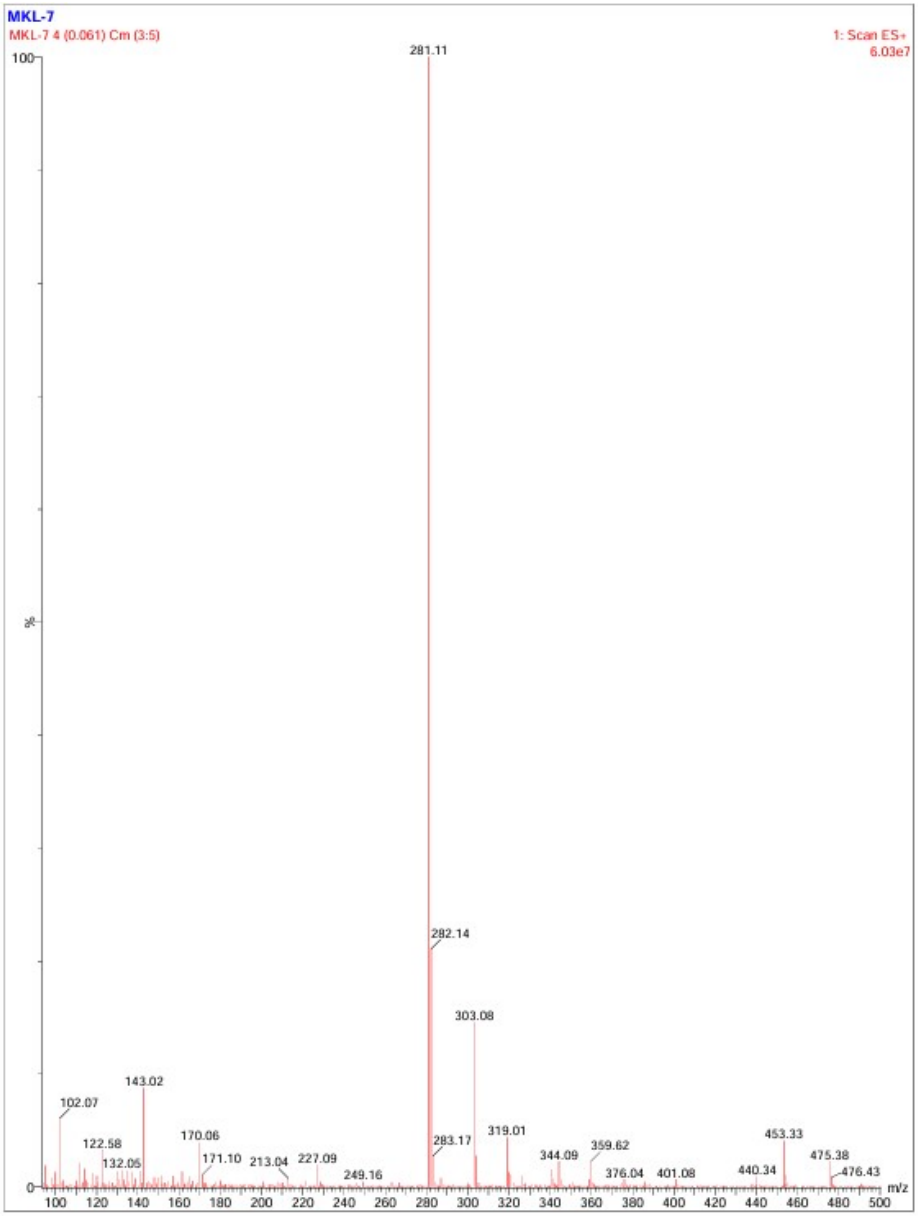

Figure S7: Mass spectrum of **HMC**

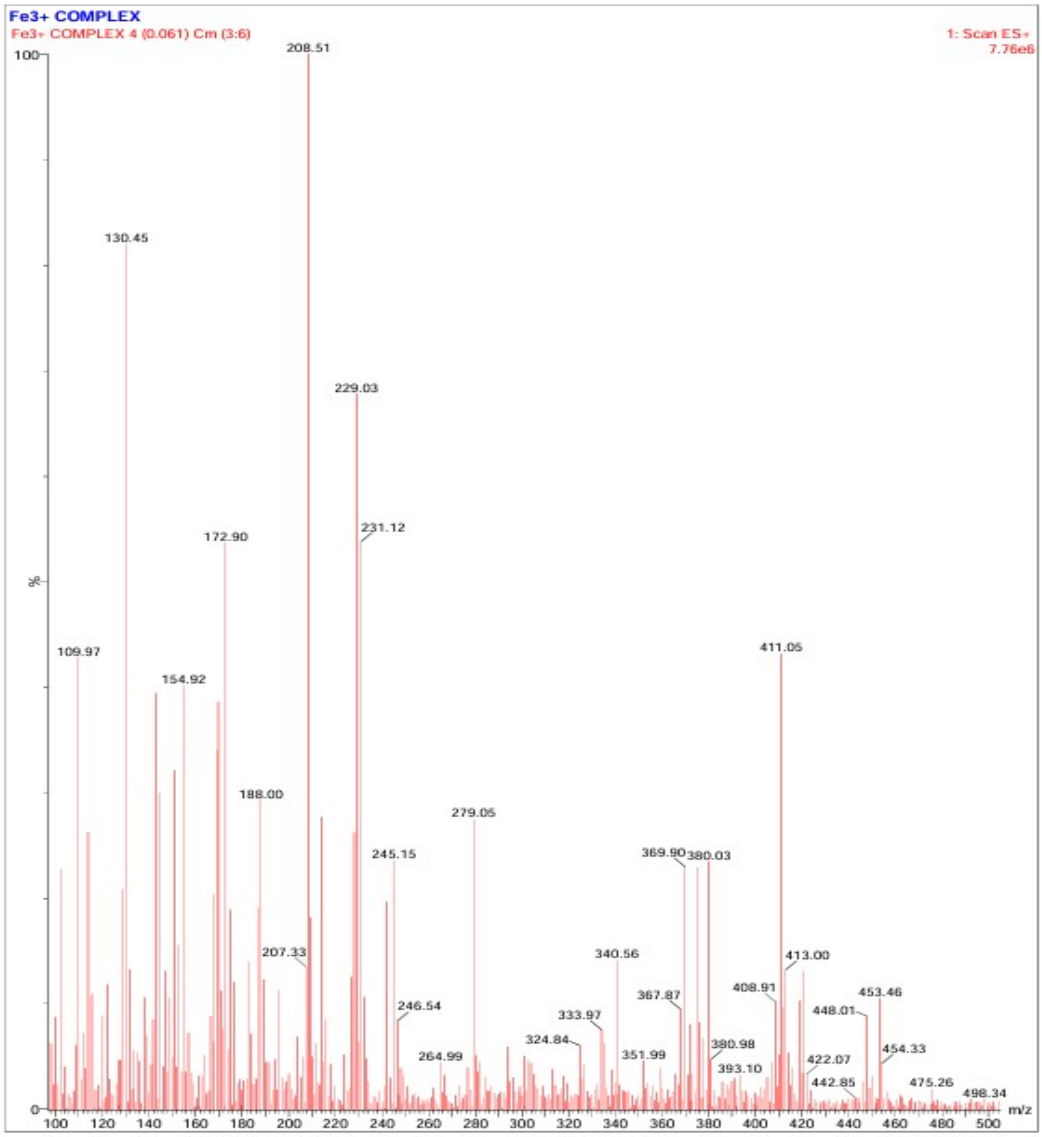

Figure S8: Mass spectrum of **HMC + $FeCl_3$**

5. Determination of Quantum yield

Here, the quantum yield φ was measured by using the following equation,

$\varphi_x = \varphi_s (Fx / F_s) (As / A_x) (n_x^2 / n_s^2)$

Where,

X & S indicate the unknown and standard solution respectively, φ = quantum yield,

F = area under the emission curve, A = absorbance at the excitation wave length,

n = index of refraction of the solvent. Here φ measurements were performed using anthracene in ethanol as standard [φ = 0.27] (error ~ 10%).

6. Soil Analysis

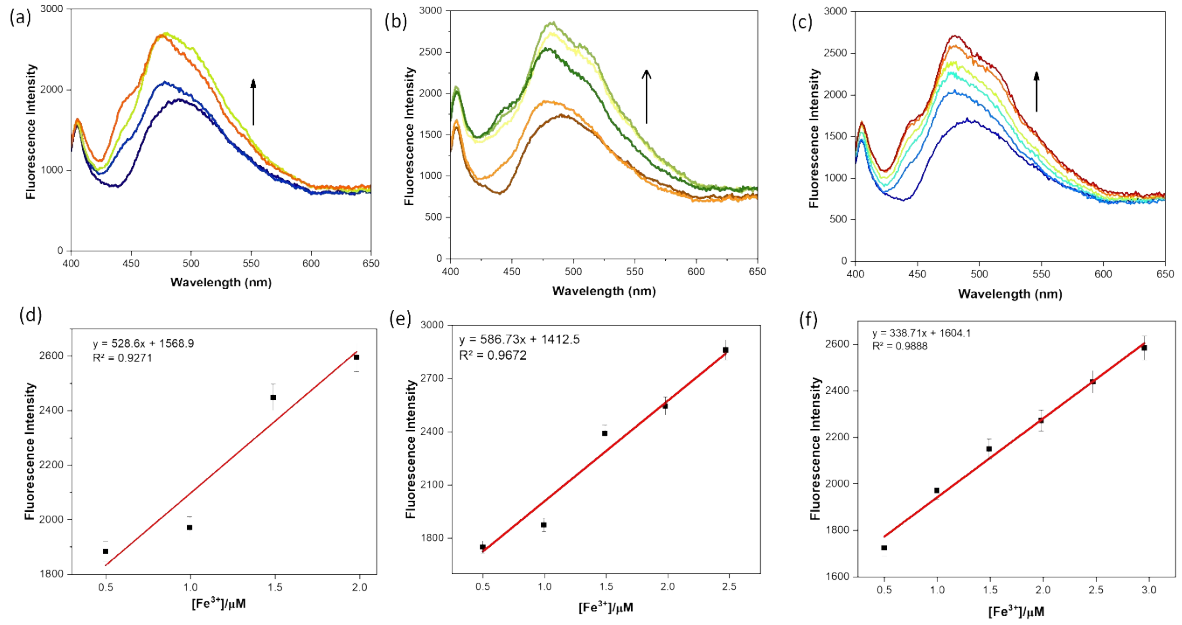

Figure S9: (a), (b) and (c) represent the fluorescence spectra observed with Field, Clay and Sand soil. Changes in fluorescence intensity of HMC as a function of [Fe^{3+}] in different soil samples. (d) Field soil (e) Clay soil (f) Sand soil

The detection limits (DL) of **HMC** with Fe^{3+} for all the soil samples were determined from the following equation:

DL = K* Sb1/S

Where K = 2 or 3 (we take 3 in this case); Sb1 is the standard deviation of the blank solution; S is the slope of the calibration curve.

From the fluorescence titrations, the Sb1 values for the Field, Sand and Clay soil are found to be 0.2108, 0.1088, and 0.1628, respectively & the corresponding slope values are 528.6, 338.71 and 586.73. The detection limits of the Field, Sand and Clay soil are calculated to be 0.0012 μM , 0.001μM, 0.0008μM.

Water sample	**Added Fe^{3+}(μM)**	**Found Fe^{3+} (μM)**	**Recovery (%)**
Field Soil	0.5013	0.6015	119
	0.9955	0.7682	77.16
	1.4897	1.667	111
	1.947	1.983	98.1
Sand Soil	0.5011	0.579	115
	0.9933	0.798	80.3
	1.488	1.667	112

	1.978	1.9391	98
	2.47	2.47	100
Clay Soil	0.4988	0.362	72.57
	338.71	372.63	110
	1.484	1.62	109
	1.98	1.97	99.4
	2.47	2.47	100
	2.95	2.90	98

Table S1: Determination of recovery percentage in the various soil samples

7. Computational details

Methods for DFT

Density Functional Theory (DFT)[2] calculations were conducted using the Gaussian 09 (Revision A.02) package, with "Gauss View" utilized for visualizing molecular orbitals. Becke's three-parameter hybrid-exchange functional, the Lee-Yang-Parr expression for nonlocal correlation, and the Vosko-Wilk-Nuair 1980 local correlation functional (B3LYP) were employed in the calculation.[3] Optimization of **HMC** and single-point energy calculations in the gas phase were performed using the 6-31+(g) basis set. The Lanl2dz basis set was used for Fe^{3+} and for H atoms we used 6-31+(g) basis set; for C, N, O, Cl, Ni atoms we employed LanL2DZ as basis set for all the calculations. The calculated electron-density plots for frontier molecular orbitals were prepared by using Gauss View 5.1 software. All the calculations were performed with the Gaussian 09W software package.[4]

Methods for silico molecular docking studies

The three-dimensional structures of Bovine Serum Albumin (PDB id 4JK4, 2.65 Å, X-ray diffraction) protein and double helical DNA (PDB id 3K5N, 3.15 Å, X-ray diffraction) were downloaded from RCSB PDB (https://www.rcsb.org/). The structures are prepared for docking by using Swiss PDB viewer software. The molecular docking between the ligand and the target molecules (BSA and DNA) were performed by AutoDock Vina software. There three- and two-dimensional (interaction) rendering of BSA-ligand, and DNA-ligand complexes were performed by UCSF ChimeraX and Biovia Discovery Studio 2024, respectively.

8. Materials and methods:

8.1 Reagents:

Dulbecco's modified Eagle's medium (DMEM), andfoetal bovine serum (FBS), were purchased from Gibco, Invitrogen, Carlsbad, CA. 3-(4,5 dimethyl-2-thiazolyl)- 2,5-diphenyl-tetrazolium bromide (MTT) and Antibiotic-antimycotic solutionwere obtained from Sigma Aldrich Co. St. Louis, US.

8.2 MCF-7 cell culture and maintenance:

MCF-7 Breast carcinoma cells were collected from Chittaranjan National Cancer Institute (CNCI), Kolkata. Cells were cultured in 10% foetal bovine serum (FBS) supplemented DMEM media with 100 U ml^{-1} penicillin, 10 mg ml^{-1} streptomycin and 4 mM L-glutamine under 5% CO_2 and 95% humidified atmosphere at 37˚C in CO_2 incubator.

8.3 *In-vitro* anticancer activity:

8.3.1: Cytotoxicity study on MCF-7 cells by MTT assay:

Dose dependent cytotoxic effect of HMC on MCF-7 cell viability after 24-hour treatment period was determined by 3-(4, 5-dimethylthiazol-2-yl)-2S-diphenyltetrazolium bromide (MTT) assay. DMEM media (0.1 ml) containing 1×10^5 cells were sub-cultured in a 96-well plate and maintained overnight in standard CO_2environment. Different concentrations (7.81, 15.62, 31.25, 62.5, 125, 250, 500 µg/ml) of HMC and 5-FU (as standard anticancer agent) were added to respective well and incubated for 24 hours. Then, 10 µl MTT solution (0.5%) was added and incubatedadditionally for 3h at 37°C and resultant purple-coloured formazan precipitate was solubilised by 100 µl DMSO. The optical density of treated and untreated cells was measured at 570 nm by Microplate reader (Bio-Rad, Model 680) and the percentage of viable cells werecalculated by following formula:

$$\text{Percentage of viable cells} = \frac{(Optical\ density\ of\ sample\ well)}{Optical\ density\ of\ untreated\ well} \times 100$$

8.3.2: Fluorescence imaging study:

The fluorescence emission pattern of HMC in presence of metallic Fe^{3+} was determined on MCF-7 breast cancer cells by fluorescence microscopic imaging. Briefly, 1×10^6 cells

were cultured in 1 ml DMEM media in sub-culture petridish and treated with HMC (concentration 50 µg/ml) for a period of 6 hours. To study changes in fluorescence emission pattern, further 1 hour incubation with 10 µM exogenous Fe^{3+} were performed and microscopic images of treated and untreated MCF-7 cells captured. Untreated cells were used as negative control. The cells were washed with phosphate buffered saline and a Leica DFC 295 microscope (Germany) was used to visualise cells by UV excitation filter.

Table S2: Comparison table of Probe **HMC** with reported Fe^{3+} sensing probes

Sl. No	Ligands	Analytes	Fluorescence Response	Detection limit	Applications	Ref
1.	**PEBD** (Pyrene-based) 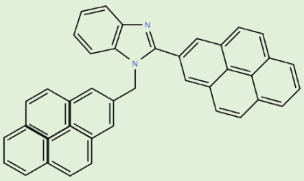	Fe^{3+}	Fluorescence quenching (Turn-off) at 440 nm	1.81 µM	Detection of Fe^{3+} in aqueous medium and drinking water	6
2.	**SS1 & SS2** (Cyanoimidazopyridine-based) 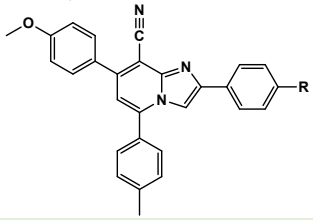	Fe^{3+} Fe^{2+} Cu^{2+}	Fluorescence quenching (Turn-off) at 470 nm	Fe^{3+} 36.64 µM (SS1), 14.33 µM (SS2)	Real-time detection using coated filter paper strips	7
3.	**APSB** (Pyrene-anthracene hybrid) 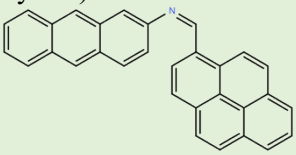	Fe^{3+}	Fluorescence enhancement (Turn-on, at 520 nm	1.95 nM	Live-cell imaging (HeLa cells): cell permeability studies, molecular logic gate functioning	8
4.	**DBQA** (Schiff-base) 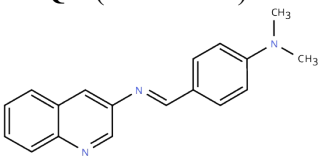	Fe^{3+} NH_3	Ratiometric response (Shift from 413 nm to 463 nm)	Fe^{3+}: 0.4 μM NH_3: 0.6 μM	Anticancer activity (HCT116 colon cancer cells),	9

5.	**DQC** (Quinoline-based with phthalimide) 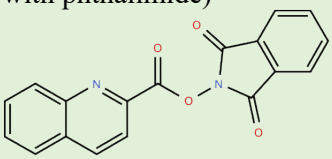	Fe^{3+}	Fluorescence quenching (Turn-off) at 400 nm	0.16 µM	Selective and sensitive recognition of Fe^{3+} in DMSO/H2O	10
6.	**HL6** (Rhodamine-based)	Fe^{3+}, HSA	Fluorescence enhancement 554 nm	0.11 µM	Cell imaging	11
7.	Oxadiazole Schiff base 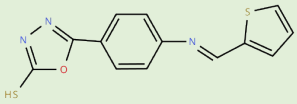	Fe^{3+}, DNA	Fluorescence quenching (Turn-off) at 408 nm	0.113 µM	In vitro Antifungal Activity	12
8.	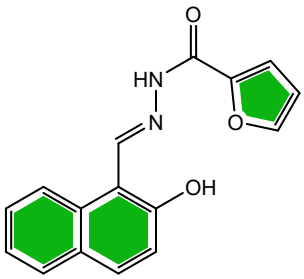	**Fe^{3+}, ct-DNA, BSA (Multi-functional probe)**	**Fluorescence Turn-On - (472 nm)**	**Fe^{3+}- 1.86 µM ct-DNA- 4.92 µM BSA- 4.8×10^{-3}µM**	***In-vitro* anticancer activity Fluorescence imaging study *Real-time analysis – Soil Analysis***	Present work

10. References:

1. R. G. Parr and W. Yang, *Density Functional Theory of Atoms and Molecules*, Oxford University Press, Oxford, 1989.
2. (a) A. D. Becke, J. Chem. Phys., 1993, 98, 5648. (b) C. Lee, W. Yang and R. G. Parr, Phys. Rev. B, 1998, 37, 785.
3. M. J. Frisch, G. W. Trucks, H. B. Schlegel, G. E. Scuseria, M. A. Robb, J. R. Cheeseman, G. Scalmani, V. Barone, B. Mennucci, G. A. Petersson, H. Nakatsuji, M. Caricato, X. Li, H. P. Hratchian, A. F. Izmaylov, J. Bloino, G. Zheng, J. L. Sonnenberg, M. Hada, M. Ehara, K. Toyota, R. Fukuda, J. Hasegawa, M. Ishida, T. Nakajima, Y. Honda, O. Kitao, H. Nakai, T. Vreven, J. A. Montgomery Jr., J. E. Peralta, F. Ogliaro, M. Bearpark, J. J. Heyd, E. Brothers, K. N. Kudin, V. N. Staroverov, R. Kobayashi, J. Normand, K. Raghavachari, A. Rendell, J. C. Burant, S. S. Iyengar, J. Tomasi, M. Cossi, N. Rega, J. M. Millam, M. Klene, J. E. Knox, J. B. Cross, V. Bakken, C. Adamo, J. Jaramillo, R. Gomperts, R. E. Stratmann, O. Yazyev, A. J. Austin, R. Cammi, C. Pomelli, J. W. Ochterski, R. L. Martin, K. Morokuma, V.

G. Zakrzewski, G. A. Voth, P. Salvador, J. J. Dannenberg, S. Dapprich, A. D. Daniels, Ö. Farkas, J. B. Foresman, J. V Ortiz, J. Cioslowski and D. J. Fox, Gaussian Inc., 2009, Wallingford CT.

4. Chaudhuri AD, Mondal S, Mahata R, Manna S, Majumder A, Dey SK, Giri D, Roy T, Baral RN, Roy S, Saha B. Folate receptor-targeted and pH-tunable dextran modified geraniol-protein nano-scaffolds stir up oxidative assault and apoptotic killing of HCT-116 colorectal cancer cells. International Journal of Biological Macromolecules. 2025 May 1; 306:141741.
5. Kumar MS, Pakrashy S, Manna S, Choudhury SM, Das B, Ghosh A, Seikh AH, Dolai M, Das AK. Fluorogenic selective detection of Zn 2+ using a pyrazole-ortho-vanillin conjugate: insights from DFT, molecular docking, bioimaging and anticancer applications. Analytical Methods. 2025;17(9):2125-33.
6. P. Rasin, M. M. Mathew, V. Manakkadan, V. N. V. Palakkeezhillam and A. Sreekanth, *J Fluoresc*, 2022, **32**, 1229–1238.
7. S. Sasan, T. Chopra, A. Gupta, D. Tsering, K. K. Kapoor and R. Parkesh, *ACS Omega*, 2022, **7**, 11114–11125.
8. P. Rasin, V. Manakkadan, V. N. Vadakkedathu Palakkeezhillam, J. Haribabu, C. Echeverria and A. Sreekanth, *ACS Omega*, 2022, **7**, 33248–33257.
9. M. Mustufa, A. Abbasi, S. Hanif, Z. U. H. Bhat, H. Kabeer, M. J. Alam, M. Ahmad and M. Shakir, *Chemistry of Inorganic Materials*, 2023, **1**, 100011.
10. P. Madhu and P. Sivakumar, *J. Mol. Struct.*, 2019, **1193**, 378–385.
11. R. Bhowmick, A. S. M. Islam, U. Saha, G. Suresh Kumar and M. Ali, *New J. Chem.*, 2018, **42**, 3435–3443.
12. R. Mehandi, R. Sultana, S. Ahmedi, M. Rana, N. Manzoor, S. Javed, Rahisuddin and N. Nishat, *J Fluoresc*, 2023, **33**, 751–772.